Pertanika J. Sci. & Technol. 6(2): 95 - 105 (1998)
ISSN: 0128-7680

Microstructural and Dielectric Properties of Ni-Zn and Li-Ni-Zn Ferrites by Impedance Spectroscopy

Mustaffa Hj. Abdullah and Ahmad Nazlim Yusoff
Physics Department
Faculty of Physical and Applied Sciences
Universiti Kebangsaan Malaysia
43600 UKM Bangi, Selangor Darul Ehsan, Malaysia

Received 23 September 1997

ABSTRAK

Bahagian-bahagian nyata dan khayalan bagi impedans kompleks dan sudut kehilangan (δ) ferit-ferit $Ni_{0.5}Zn_{0.5}Fe_2O_4$ dan $(Li_{0.5}Fe_{0.5})_{0.5}Ni_{0.2}Zn_{0.3}$ Fe_2O_4 diukur pada 300 K dalam julat frekuensi 1 - 10 MHz menggunakan penganalisis rangsangan frekuensi. Spektrum impedans satah-kompleks bagi sampel-sampel tersebut dikaitkan dengan litar-litar setara yang terdiri daripada unsur-unsur berintangan dan berkapasitans daripada komponen-komponen pukal (butiran) dan sempadan butiran. Impedans ukuran dan simulasi dianalisis menggunakan kaedah penyesuaian kuasa-dua terkecil kompleks taklinear. Komponen-komponen yang disimulasi untuk litar yang berkenaan ditafsirkan sebagai parameter-parameter cirian bagi sifat-sifat mikrostruktur bahan. Sifat mikrostruktur dilengkapi dengan kajian morfologi menggunakan mikroskop imbasan elektron. Sifat dielektrik pada rantau-rantau frekuensi rendah dan tinggi ditafsirkan sebagai berpunca masing-masing daripada pengutuban antaramuka dan orientasi. Suatu rantau kapasitans negatif pada frekuensi rendah dicerap untuk kedua-dua sampel. Kebergantungan frekuensi parameter-parameter cirian bagi komponen-komponen mikrostruktur dan sifat dielektrik bahan-bahan ferit yang berkenaan dibincangkan.

ABSTRACT

The real and imaginary parts of the complex impedances and the loss angle (δ) of $Ni_{0.5}Zn_{0.5}Fe_2O_4$ and $(Li_{0.5}Fe_{0.5})_{0.5}Ni_{0.2}Zn_{0.3}$ Fe_2O_4 ferrites were measured at 300 K in the frequency range of 1 - 10 MHz using a frequency response analyser. The complex - plane impedance spectra of the samples are associated with equivalent circuits composed of resistive and capacitive elements due to the bulk (grain) and the grain boundary components. The measured and simulated impedances were analysed using the complex nonlinear least square (CNLS) fitting method. The simulated components of the circuit are interpreted as the characteristic parameters of the microstructural properties of the materials. Microstructural properties are complemented by a morphological study using a scanning electron microscope. The dielectric properties at low and high frequency regimes are interpreted as mainly due to the interfacial and orientational polarizations respectively. A region of negative capacitances at low frequencies is observed for both samples. Frequency dependence of the characteristic parameters of the microstructural components and the dielectric behaviour of the materials are discussed.

Keywords: ferrites, complex impedance, polarization, dielectric properties, impedance spectroscopy

INTRODUCTION

It is known that given an impedance (or admittance) spectrum of a material, one can calculate the resistive and the capacitive components of an equivalent circuit that is responsible for it (Armstrong *et al.* 1978; Archer and Armstrong 1978; Straton *et al.* 1979; Bayard 1979; Badwal 1988; Yeh and Tseng 1989; Yusoff and Abdullah 1995; Abdullah and Yusoff 1996). Each of the circuit components represents a specific phenomenon, either due to the bulk (grain) or one of the various interface processes resulting from the response of the material to the applied alternating electric field. In polycrystalline materials, the different contributions can be distinguished since the complex-plane impedance spectrum is usually analysed into two or more distinguishable profiles, normally in the form of semicircular diagrams, due to the difference in the time constants for the different processes. Hence, the characteristic properties associated with the microstructural components can be investigated in detail. Dielectric quantities, such as dielectric constant and dielectric loss, can be directly evaluated from the real and imaginary parts of the complex impedance and the geometry of the samples. The complex impedance and the dielectric quantities are complementary in investigating the dielectric behaviour of materials. Hence, a complete characterization and understanding of the dielectric properties of the materials can be made.

The spinel ferrites, assumed to be in their stoichiometric compositions and structurally defectless, should be pure ionic insulators with small dielectric constants and dielectric losses which are insensitive to the change in frequency and temperature. The polarizability in the materials then would be solely from atomic and electronic polarization mechanisms. However, the inherent existence of the mixed valence states of some of their metallic ion components, as well as their formation during the process of preparation, and the existence of defect in the form of vacancy, results in electrical and dielectric behaviour which are dependent on frequency and temperature. Previous works (Reddy and Rao 1985; Miroshkin *et al.* 1990; Abdullah and Yusoff 1996, 1997) showed that the dielectric constants of ferrite materials are very large over a wide range of frequencies. The dielectric properties of some ferrites in the low frequencies have been discussed as due to interfacial polarization (Prakash and Baijal 1985; Suryavanshi *et al.* 1991; Kuanr and Srivastava 1994; Abdullah and Yusoff 1996). In other reports, the complex-plane representations of ε'' versus ε' or Cole-Cole (CC) plots in a certain frequency range resemble a semicircle or two partially overlapping semicircles which are partially depressed to below the ε' axis (Murthy *et al.* 1989; Miroshkin *et al.* 1990). The recent view on the dielectric properties of some ferrites by the present authors (Abdullah and Yusoff 1997) is that based on the universal relaxation law (Jonscher 1983, 1991, 1995).

The techniques of impedance spectroscopy have been widely used to study the characteristics of solid state electrolytes and ceramic oxides (Armstrong *et al.* 1978; Archer and Armstrong 1978; Straton *et al.* 1979; Bayard 1979; Badwal 1988; Yeh and Tseng 1989). However, the application of this technique to study the properties of magnetic ceramics is lacking. This paper is a continuation of our earlier works on the use of this technique for some ferrite materials (Yusoff and Abdullah 1995; Abdullah and Yusoff 1996, 1997) in studying the microstructural and dielectric properties of the materials. In this work, the simulation of the impedance data is improved with the use of complex nonlinear least square (CNLS) fitting method in order to obtain the best values of the relevant physical parameters.

MATERIALS AND METHODS

Samples of $Ni_{0.5}Zn_{0.5}Fe_2O_4$ (NiZn) and $(Li_{0.5}Fe_{0.5})_{0.5}Ni_{0.2}Zn_{0.3}Fe_2O_4$ (LiNiZn) were prepared by a conventional double sintering technique from high purity powders of Li_2O (99.99%), NiO, ZnO and Fe_2O_3 (99.999%). For NiZn ferrite, the thoroughly mixed and ground powders were sintered at 1030°C and 1230 °C for 6 h and 15 h respectively, while for LiNiZn, the powders were sintered at 800°C and 1050°C for 6 h and 15 h respectively. A small amount of Bi_2O_3 (0.5 weight %) was added to the starting powders for LiNiZn ferrite, which then acted as fluxing agent. In all cases, pellets of 13 mm and 2 mm in diameter and thickness were made at a pressure of 50 MPa with a small amount of polyvinyl alcohol (PVA) as a binder. The formation of a single-phase cubic spinel structure for all compositions was confirmed from X-ray analysis (Siemens D5000 Diffractometer). A morphological study was made by a scanning electron microscope (Philips XL-30).

A frequency response analyser (HFRA Model HF 1255) was used in the measurements of the real (Z') and imaginary (Z") parts of the complex impedance ($Z^* = Z' - jZ''$) in the frequency range of 1 - 10 MHz at 300 K. Details of the experimental techniques have been described elsewhere (Yusoff and Abdullah 1995; Abdullah and Yusoff 1997). The quantities obtained from the measurements are Z', Z" and the loss angle $\delta = 90 - \theta$, where θ is the phase difference between the input and the output signals. The complex dielectric permittivitiy of the materials is $\varepsilon^* = \varepsilon' - j\varepsilon''$, where the real dielectric permittivity (ε') and the dielectric loss (ε'') were evaluated from the impedance data and the dimensions of the materials. Details of the calculation of the dielectric quantities have been given elsewhere (Yusoff and Abdullah 1995; Abdullah and Yusoff 1997). The results for different compositions are represented as the plots of $\varepsilon'_r = \varepsilon''_r = \varepsilon''/\varepsilon_o$ and tan δ versus frequency in logarithmic scales, where ε_o is the permittivity of the free space.

The impedance data were analysed using a complex nonlinear least square fitting method. The fitting criteria were the smallest values of the target function (χ^2) and the standard deviation (σ^2), where $\chi^2 = \Sigma([(Z_{ei} - Z_{si})^2/Z_{si}]$ and $\sigma = \sqrt{(1/N)\ \Sigma[(Z_{ei} - Z_{si})^2]}$, with $\chi'^2 = \Sigma[(Z'_{ei} - Z'_{si})^2/Z'_{si}]$, $\chi''^2 = \Sigma[(Z''_{ei} - Z''_{si})^2/Z''_{si}]$, $\sigma' = \sqrt{(1/N)\ \Sigma[(Z'_{ei} - Z'_{si})^2]}$ and $\sigma'' = \sqrt{(1/N)\ \Sigma[(Z''_{ei} - Z''_{si})^2]}$. Z'_{ei} and Z''_{ei} are the real and imaginary components of the impedance for ith experimental data at frequency ω_i, while Z'si and Z''_{si} are the simulated values of those quantities. The simulated data are obtained from the proposed model for impedance response as discussed in the later sections.

RESULTS AND DISCUSSION

Fig. 1 shows the measured complex-plane resistivity spectra of the NiZn and LiNiZn ferrites. As described above, the complex resistivity plot is the plot of specific complex impedance (impedance per unit length and cross-sectional area), which is useful if various parameters from different samples are to be compared. The profiles of the resistivity and impedance plots are exactly the same. In the following discussion the specific values of Z' and Z'' (ρ' and ρ'') are referred to as impedances. It can be seen that the profile of the impedance diagrams for NiZn and LiNiZn ferrites is composed of two overlapping semicircles, and in both cases the semicircles are depressed to below the Z' axis. The impedance response in polycrystalline materials is normally comprised of the bulk (grain), the grain boundary and the material-electrodes interface processes in order of decreasing frequency. However, the impedance responses from the bulk and the grain boundary will overlap each other if the time constants that characterize the two processes are the same. Kleitz and Kennedy (1979) reported that the impedance semicircles will be overlapped significantly if the time constant of the different processes differs by a factor of less than 100. The interpretation of the impedance semicircles as due to the response of the material in the present result is substantiated by the fact that the use of different materials for electrodes or holder, such as copper or silver, has no effect on the profile and range of the semicircular arc along the Z' axis. A small effect on the shift of the arc along the Z' axis is observed as expected, since the series resistance tends to be variable for different contact materials.

An equivalent circuit for the complex impedance dispersion of the ferrites is shown in *Fig. 1(c)* where Rb and Cb represent the components due to the bulk process, while Rg and Cg are due to the grain boundary process. The complex impedance of the circuit is then effectively equal to the Cole-Cole impedance distribution expression (1) by using the parameters as sketched ideally in *Fig 1(d)*. Thus, the Cole-Cole expression for the two overlapping semicircles is given by

$$Z^*(\omega) = R_s + \frac{R_b}{1 + (j\omega\tau_{ob})^{1-\alpha b}} + \frac{R_g}{1 + (j\omega\tau_{og})^{1-\alpha g}} \tag{1}$$

where

$$Z'(\omega) = R_s + \frac{R_b[1 + (\omega\tau_{ob})^{1-\alpha b}\sin(\alpha_b\pi/2)]}{1 + (2\omega\tau_{ob})^{1-\alpha b}\sin(\alpha_b\pi/2) + (\omega\tau_{ob})^{2(1-\alpha b)}} + \tag{2}$$

$$\frac{R_b[1 + (\omega\tau_{ob})^{1-\alpha b}\sin(\alpha_g\pi/2)]}{1 + (2\omega\tau_{ob})^{1-\alpha b}\sin(\alpha_b\pi/2) + (\omega\tau_{og})^{2(1-\alpha g)}}$$

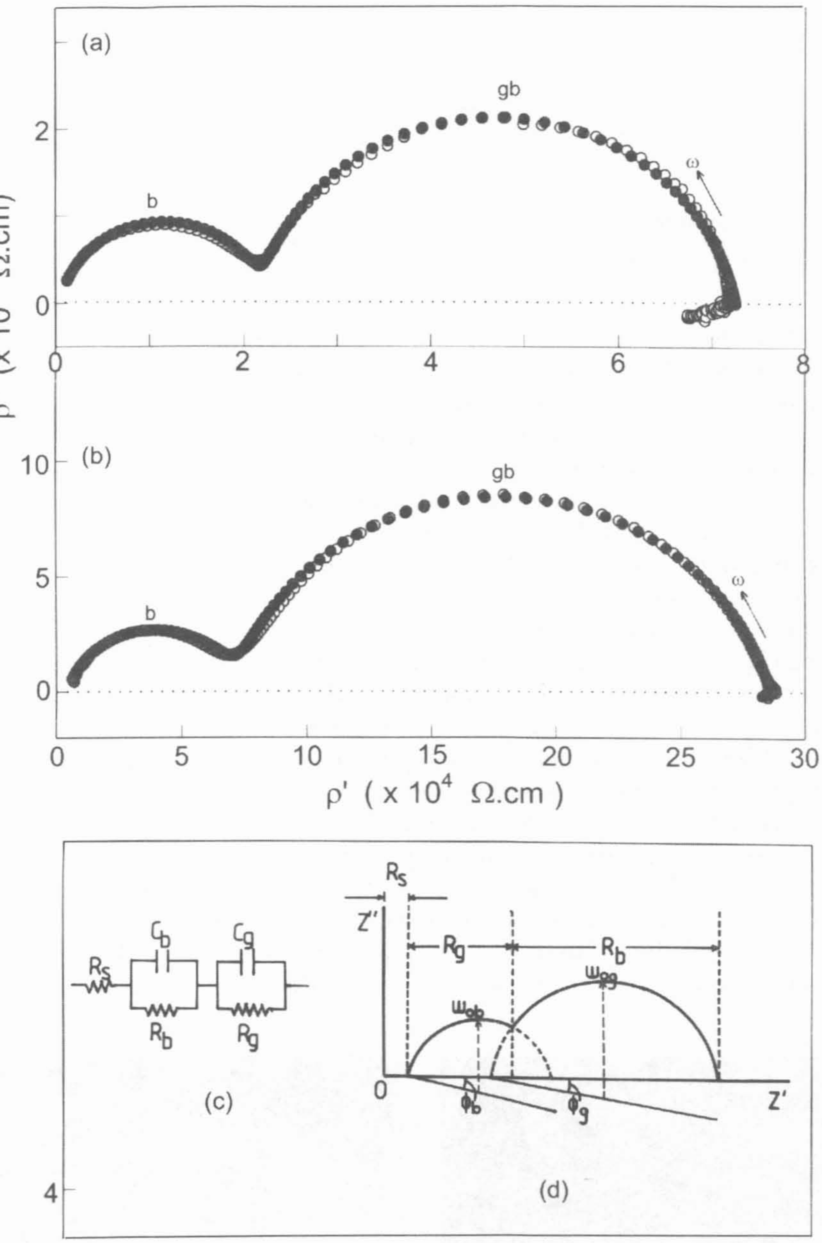

Fig. 1. Complex-plane resistivity spectra for (a) $Ni_{0.5}Zn_{0.5}Fe_2O_4$ and (b) $(Li_{0.5}Fe_{0.5})_{0.4}Ni_{0.2}Zn_{0.3}Fe_2O_4$ ferrites from experiment (o). Simulated plot using CNLS fitting method is indicated by the filled circles. On the scales used in the plots, the measured and simulated points overlap. In the diagrams, g and gb denote the arcs due to the bulk and grain boundary respectively. (c) A proposed equivalent circuit and (d) A sketch of complex-plane impedance spectrum showing various parameters used in the simulation.

and

$$Z''(\omega) = \frac{R_b(\omega\tau_{ob})^{1-\alpha b}\cos(\alpha_b\pi/2)}{1+(2\omega\tau_{ob})^{1-\alpha b}\sin(\alpha_b\pi/2)+(\omega\tau_{ob})^{2(1-\alpha b)}} +$$

$$\frac{R_b(\omega\tau_{ob})^{1-\alpha b}\cos(\alpha_b\pi/2)}{1+(2\omega\tau_{og})^{1-\alpha g}\sin(\alpha_b\pi/2)+(\omega\tau_{og})^{2(1-\alpha g)}} \quad (3)$$

In the above equations, α_b and α_g are the depression parameters which measure the deviation of the impedance plot from the ideal Debye type of response for the bulk and grain boundary respectively. The relation between the depression angles (ϕ_b and ϕ_g) and depression parameters (α_b and ϕ_g) can be written as $\alpha_b = 2\phi_b/\pi$ and $\alpha_g = 2\phi_g/\pi$. The value of α_b and α_g lie between 0 and 1 as the possible values of ϕ_b and ϕ_g are in the range of 0° an 90°, where $\alpha_b = \alpha_g = 0$ is the case of the ideal impedance distribution. R_b and R_g are the simulated values for the grain and grain boundary resistances. The mean relaxation times for the grain and grain boundary processes, $\tau_{ob} = R_bC_b$ and $\tau_{ob} = R_gC_g$, are the inverse of the peak frequencies, ω_{ob} and ω_{og}, respectively, so that C_b and C_g can be evaluated.

The experimental and simulated data were then analysed further using the complex nonlinear least square fitting method in order to obtain the best fit. The best simulated plot using the CNLS criteria is also shown in *Fig. 1* for all samples. Table 1 shows various simulated parameters obtained from the CNLS fitting procedure. The agreement between the measured and simulated impedance diagrams is good for all cases. Therefore, the proposed equivalent circuits correctly represent the impedance characteristic of the materials, and the components of the circuit are the associated values of the physical parameters that describe their microstructural properties. *Plate 1* shows the SEM micrographs of the Ni-Zn and the Li-Ni-Zn ferrites respectively. In general, the ferrites are granular and polycrystalline. It can be seen that the Ni-Zn ferrite is denser with

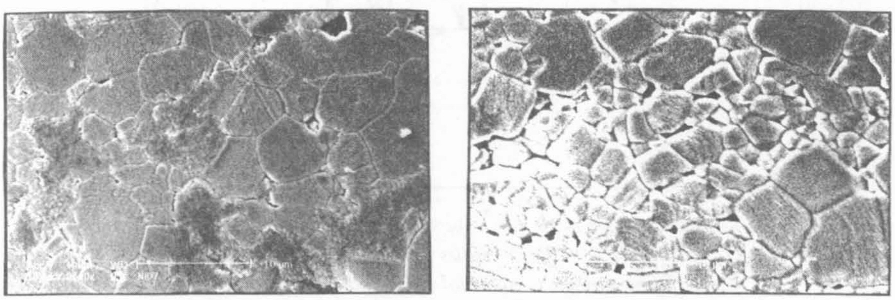

a b

Plate 1. Micrographs for (a) $Ni_{0.5}Zn_{0.5}Fe_2O_4$ and (b) $(Li_{0.5}Fe_{0.5})_{0.4}Ni_{0.2}Zn_{0.3}Fe_2O_4$ ferrites at 2500 magnification

TABLE 1
Magnitude of various microstructural parameters at 300 K for the ferrites $Ni_{0.5}Zn_{0.5}Fe_2O_4$ and $(Li_{0.5}Fe_{0.5})_{0.4}Ni_{0.2}Zn_{0.3}Fe_2O_4$, which are denoted by NiZn and LiNiZn respectively. Direct current resistivity ((dc) was measured using an electrometer (model Keithley 619)

	Ferrite samples	
	NiZn	LiNiZn
$R_s \pm 10$ (Ω)	100	1020
$\rho_{dc} \pm 0.001$ (x 10^4 Ω cm)	7.609	23.900
$\rho_b \pm 0.001$ (x 10^4 Ω cm)	0.440	6.711
$\rho_g \pm 0.001$ (x 10^4 Ω cm)	4.600	19.609
$C_b \pm 0.001$ (pF)	0.230	4.285
$C_g \pm 0.001$ (nF)	1.611	0.955
$\omega_{ob} \pm 10$ (rad s^{-1})	9867110	3482900
$\omega_{og} \pm 10$ (rad s^{-1})	13490	5340
$\phi_b \pm 0.5$ (deg.)	13.0	13.0
$\phi_g \pm 0.5$ (deg.)	6.0	11.0
$\alpha_b \pm 0.005$	0.145	0.145
$\alpha_g \pm 0.005$	0.065	0.120
$\tau_{ob} \pm 0.005$ (x 10^{-6} s)	0.010	0.287
$\tau_{og} \pm 0.005$ (x 10^{-3} s)	0.070	0.190

finer grain boundaries, whereas the Li-Ni-Zn ferrite has smaller grains with more voids. The latter microstructure is consistent with a larger grain boundary resistivity and the overall d.c. resistivity of the ferrite. For both samples, the impedance spectrum shows a region of negative impedances at low frequencies in the range of 1 MHz - 1 Hz. This region is not represented in the equivalent circuit. This characteristic is discussed in relation to the dielectric properties of the materials in the following sections.

Fig. 2 shows the frequency dependence of the dielectric constant (ε'_r) and the dielectric loss (ε''_r) in the range of 1 - 10 MHz for the samples. The variation of ε' and ε''_r with frequency indicates the existence of several different processes dominating within different frequency ranges. The results for all compositions show that a behaviour analogous to the Debye relaxation process is dominant at high frequencies above 1 MHz. There is an indication of the existence loss peak at about 10 MHz for both samples. However, this is strongly influenced by the appearance of interfacial polarization process at the low frequency end. Debye relaxation is associated with orientational polarization from $Fe^{3+} - Fe^{2+}$ dipoles. Rotational displacements of the dipoles may be viewed as the exchange of electrons between the ions when subjected to the alternating electric field. The dipole moments in ferrites may also be due to the association of the occupied cations with the positive ions vacancies, so that the cations and the vacancies can exchange positions on applying the electric field. Both ε'_r and ε''_r increase sharply with decreasing frequency after a critical frequency (f_c) that

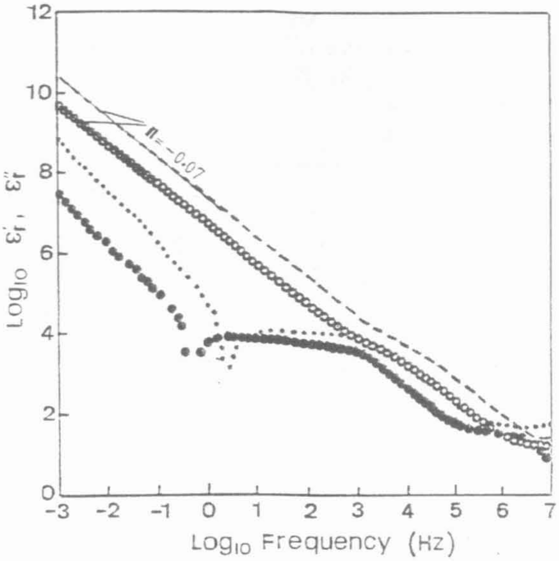

Fig. 2. Plots of dielectric constant and dielectric loss (ε'_r and ε''_r) versus frequency in the range of 1 - 10 MHz for the ferrites $Ni_{0.5}Zn_{0.5}Fe_2O_4$ (• and -----) and $(Li_{0.5}Fe_{0.5})_{0.4}Ni_{0.2}Zn_{0.3}Fe_2O_4$ (● and ○). The negative values of dielectric constant for the samples (• and ●) are plotted as $|\log_{10} \varepsilon'_r|$. The exponents n are derived from the slope = n -1.

corresponds to the intersection between ε'_r and ε''_r at the low frequency end of the Debye-like region. The values of fc for NiZn and LiNiZn were found to be about 2 MHz and 1 MHz respectively. *Fig. 2* shows that the Debye contribution at 1 MHz to the real dielectric permittivity of the ferrites is only about 1% of the interfacial contribution at 1 kHz. In the linear plot of the impedance spectrum, the value is too small to be distinguishable. Therefore, it is not represented in the equivalent circuit model. The proposed two-layer C-R components are interpreted to present the dominant interfacial polarization resulting from the grain and grain boundary components of the materials. The steep rise of ε'_r and ε''_r is associated with interfacial relaxation. It seems that the region between 1 - 100 kHz is dominated by interfacial polarization. Interfac al polarization is due to the existence of an interfacial barrier between two relatively conducting regions. This corresponds to the frequency region where the impedance response is dominated by the grain boundary process. It is known that hopping electrons between Fe^{3+} and Fe^{2+} ions may be trapped by various barriers in the form of structural inhomogeneities so as to produce interfacial polarization. However, the extent of interfacial characteristics is limited due to the appearance of negative capacitance at frequencies below about 1 Hz. The negative capacitances, which lead to negative ε'_r, appear when the impedance plot dips below the real Z' axis. According to Jonscher (1995), the ideal low frequency dispersion for dielectric permittivity can be represented by $\varepsilon^*_r = A(j\omega)^{n-1}$, where n is small and positive, which can be written as $\varepsilon^*_r = A[\sin(n\pi/2) - j\cos(n\pi/2)]\omega^{n-1}$, so that ε'_r and $\varepsilon''_r \propto \omega^{n-1}$. The exponents n in the negative capacitance region are marginally negative, where the values are - 0.07 (slope = - 1.07) for both samples. This is the consequence of $\varepsilon''_r/\varepsilon'_r = \cot(n\pi/2)$, where n is negative if ε'_r is to be negative. Negative capacitance is associated with a rising current in the step-function time-domain response (Jonscher 1995). This effect is possibly due to nonlinear response of the ferrites at low frequencies.

The dielectric loss is mainly due to the conductivity of the materials. Hence, a sample with lower resistivity would exhibit higher loss. The conductivity in the ferrite samples depends on the concentration of Fe^{2+} ions which in conjunction with the majority Fe^{3+} ions will act as hopping sites for electron conduction. Fe^{2+} ions formed from the reduction of Fe^{3+} ions when the ferrites were heated at elevated temperature. The polarizability as represented by ε'_r for all samples also depends on the availability of the divalent and trivalent metallic cations. The polarization at low frequencies is affected by the negative capacitance; while at high frequencies the total polarization is influenced by the contribution from the cation-vacancy orientational polarization. Another meaningful representation of the dielectric loss is by $\tan\delta = \varepsilon''_r/\varepsilon'_r$, where $\delta = 90 - \theta$ is the loss angle. *Fig. 3* shows the plot of tan δ versus frequency for different compositions. For both samples, tan is δ minimum at certain frequencies. These minima occur at the frequencies that correspond to the interfacial and Debye-like relaxation processes. In general, tan δ values are smaller for ferrite with higher resistivity.

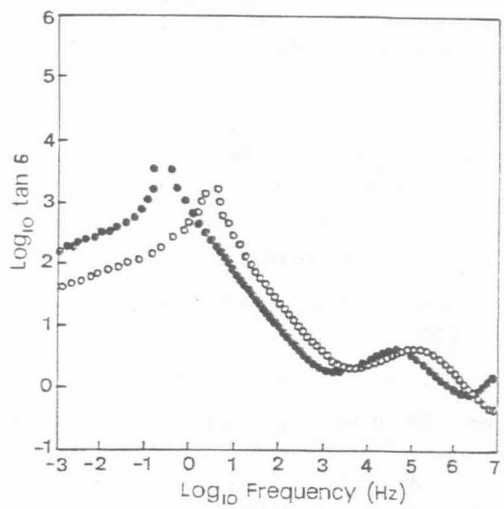

Fig. 3. Frequency dependence of loss tan δ in the range of 1 - 10 MHz for $Ni_{0.5}Zn_{0.5}Fe_2O_4$ (○) and $(Li_{0.5}Fe_{0.5})_{0.4}Ni_{0.2}Zn_{0.3}Fe_2O_4$ (●) ferrites. The negative values of log10 tan δ are plotted as $|\log_{10}\tan\delta|$.

In conclusion, the technique of impedance spectroscopy is reliable in studying the microstructural and dielectric properties of ferrite materials. Electrical parameters that characterize the microstructural components can be accurately obtained by simulation using the equivalent circuit and complex nonlinear least square method. Measurements can be done over a wide range of signal frequency.

ACKNOWLEDGEMENTS

This work is supported by the Research and Development grant IRPA 09-02-02-0005 of the Ministry of Science and Environment of Malaysia.

REFERENCES

ABDULLAH, M.H. and A.N. YUSOFF. 1996. Complex impedance and dielectric properties of an Mg-Zn ferrite. *J. Alloys and Compounds* **233**: 129-135.

ABDULLAH, M.H. and A.N. YUSOFF. 1997. Frequency dependence of complex impedance and dielectric behaviour of some Mg-Zn ferrites. *J. Mater. Sci.* **32**: 5817-5823.

ARCHER, W.I. and R.D. ARMSTRONG. 1978. The application of a.c. impedance methods to solid electrolytes. In *Electrochemistry*, ed. H.R. Thirsk, p. 157-202 and references therein. London: Chemical Society.

ARMSTRONG, R.D., M.F. BELL and A.A. METCALF. 1978. The a.c. impedance of complex electrochemical reactions. In *Electrochemistry*, ed. H.R. Thirsk, p. 99-127. London: Chemical Society.

BADWAL, S.P.S. 1988. Impedance spectroscopy and microstructural studies on materials for solid state electrochemical devices. In *Solid State Ionic Devices - Proceedings of International Seminar on Solid State Ionic Devices*, ed. B.V.R. Chowdari and S. Radhakrishna, p. 165-189. Singapore: World Scientific.

BAYARD, M.L. 1979. Analysis of the alternating current properties of lisicon ceramics. In *Proceedings of the International Conference on Fast Ion Transport in Solids, Electrodes and Electrolytes*, Lake Geneva, Wisconsin, USA, ed. P. Vashista, J.N. Mundy and G.K. Shenoy, p. 479–481. New York: North-Holland.

JONSCHER, A.K. 1983. *Dielectric Relaxation in Solids.* London: Chelsea Dielectric Press.

JONSCHER, A.K. 1991. Low-frequency dispersion in volume and interfacial situations. *J. Mater. Sci.* **26**: 1618-1626.

JONSCHER, A.K. 1995. *Universal Relaxation Law.* London: Chelsea Dielectric Press. .

KLEITZ, M. and J.H. KENNEDY. 1979. Resolution of multicomponent impedance diagrams. In *Proceedings of the International Conference on Fast Ion Transport in Solids, Electrodes and Electrolytes.* Lake Geneva, Wisconsin, USA, ed. P. Vashita, J.N. Mundy and G.K. Shenoy, p. 185-188. New York: North-Holland.

KUANR, B.J. and G.P. SRIVASTAVA. 1994. Dispersion observed in electrical properties of titanium-substituted lithium ferrites. *J. Appl. Phys.* **75**: 6115-6117.

MIROSHKIN, V.P., V.V. PASSYNKOV and K. PERSYNSKY. 1990. The influences of Mn ions on the dielectric properties of Mn-Zn ferrites. *Acta Physica Polonica* **A77**: 715-721.

MURTHY, S.S.N, V.R.K. MURTHY and J. SOBHANADRI. 1989. Anomalous dielectric behaviour of some ferrites. *J. Appl. Phys.* **65**: 2159-2161.

PRAKASH, C. and J.S. BAIJAL. 1985. Electrical conductivity and dielectric behaviour of $Fe_{2-2x}Sn_xZn_{1+x}O_4$. *J. Less-Common Met.* **114**: 241-248.

REDDY, P.V. and T.S. RAO. 1985. Dielectric behaviour of mixed Mn-Mg ferrites at low frequencies. *J. Less-Common Met.* **105**: 63-68 and references therein.

STRATON, T., A. MACHALE, D. BUTTON and H.L. TURNER. 1979. Improved electrical characterisation of ceramic oxides - bulk vs. interface effects. In *Electronic Materials*, ed. N.B. Hannay and U. Colombo, p. 71–81. New York: Plenum Press.

SURYAVANSHI, S.S., RS. PATIL, S.A. PATIL and S.R. SAWANT. 1991. D.C. conductivity and dielectric behaviour of Ti^{4+}-substituted Mg-Zn ferites. *J. Less-Common Met.* **168**: 169-174.

YEH, Y.C. and T.Y. TSENG. 1989. Analysis of the d.c. and a.c. properties of K_2O-doped porous $Ba_{0.5}Sr_{0.5}TiO_3$ ceramic humidity sensor. *J. Mater. Sci.* **24**: 2739-2745.

YUSOFF, A.N. and M.H. ABDULLAH. 1995. Complex impedance techniques and some properties of $Mn_{0.5}Zn_{0.5}Fe_2O_4$ ferrites. *J. Fiz. Mal.* **16**: 129-137.